

# Strength Reduction Technique in Stability Analysis of Jointed Rock Slopes

Reza Mahin Roosta<sup>1</sup>, Mohammad Hossein Sadaghiani<sup>2</sup>, Ali Pak<sup>3</sup>

<sup>1</sup>Assistant Professor, Zanzan University, Engineering Department, University Boulevard, P.O.Box 45195-313, Zanzan, Iran. E mail: r\_mahinroosta@yahoo.com

<sup>2</sup>Assistant Professor, Sharif University of Technology, Department of Civil Engineering, P.O. Box 11365-9313, Tehran, Iran. E mail: mhsadagh@sharif.edu

<sup>3</sup>Associate Professor, Sharif University of Technology, Department of Civil Engineering, P.O. Box 11365-9313, Tehran, Iran. E mail: pak@sharif.edu

**Abstract:** Existence of discontinuities causes higher deformability and lower strength in rock masses. Thus joints can change the rock mass behaviour due to the applied loads. For this reason properties and orientation of the joint sets have a great effect on the stability of rock slopes.

In this paper, after introducing some numerical methods for evaluating the factor of safety for the stability of slopes, stability of jointed rock slopes in the plane strain condition is investigated with the strength reduction technique; this method is modified and applied in the multilaminar framework. First of all, stability of one homogeneous rock slope is investigated and compared with the limit equilibrium method. Then stability of a layered rock slope is analyzed with some modifications in the strength reduction technique. Effects of orientation, tensile strength and dilation of layered joint sets on the factor of safety and location of the sliding block are explained.

**Keywords:** Jointed rock mass, Multilaminar Model, Numerical method, Slope stability, Strength reduction technique.

## 1- Introduction

In the limit equilibrium analysis, factor of safety (FS) is defined as the ratio of soil or rock shear strength at failure to the mobilized shear stress on the failure surface. Although this method is very simple and engineers usually use this method to analyze the stability and design the embankments and excavations, it has some disadvantages; first the stress-strain behavior of the soil or rock mass is not taken into account in the calculation of the factor of safety. Secondly shape of critical slip surface must be calculated by trial and error. Beginning of failure and its development are unknown and finally initial stresses are not considered in the limit equilibrium analysis.

Numerical stress and deformation analysis does not calculate the factor of safety directly. However, factor of safety can be

defined by taking the ratio of the calculated shear strength under failure condition to the shear stresses under given normal condition. There are two basic approaches for calculating the factor of safety with numerical methods: "shear strength reduction technique" and "enhanced limit method". The shear strength reduction technique was used to evaluate the factor of safety of slopes by Zienkiewicz et al. [1], Naylor [2], Matsui and San [3], Lane et al. [4], Dawson et al. [5] and Rachez et al. [6]. In this method, first of all initial stresses due to soil weight are calculated from gravity loading. Then, cohesion and friction angle of materials are decreased with a factor  $F$  until failure occurs in the slope, which is identified by the onset of instability in the numerical models:

$$c' = c / F \quad [1a]$$

$$\tan \varphi' = \tan \varphi / F \quad [1b]$$

With above definition, shape and position of the sliding block are developed during the numerical analysis.

The “enhanced limit method” was introduced by Naylor [2]. In this method the stresses on critical surface are calculated from numerical methods and factor of safety is determined as the ratio of ultimate loads to applied loads on the same surface:

$$FS = \frac{\int \tau_f \cdot dl}{\int \tau_n \cdot dl} \quad [2]$$

$\tau_f$  and  $\tau_n$  are shear strength and real shear stress on the infinitesimal slip surface  $dl$ , respectively. In this method some algorithms are required to find the critical surface. For example shear strain contours and velocity plots may lead to a probable critical surface (Farias and Naylor [7]).

## 2- Definition of stress level, over-stress ratio and local factor of safety

The mobilisation of shear strength at a point depends on the stress path. Each stress path may have its own value of failure. Consider principal stresses  $\sigma_1$  and  $\sigma_2$  are applied on a point. Fig. 1 shows the stress state and the corresponding Mohr circle with radius  $r_A$ .

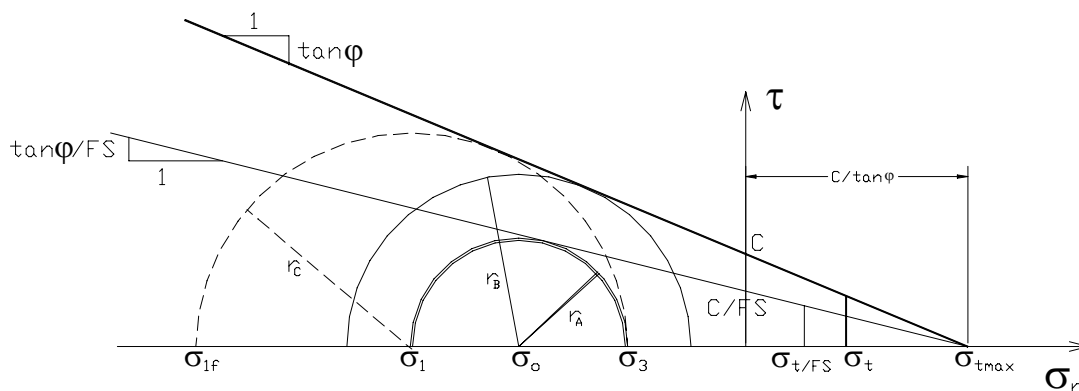


Fig. 1. Effect of stress path on failure and concept of strength reduction technique

Suppose that shear strength of material is calculated from Mohr-Coulomb criterion. One stress path is defined with constant minimum principal stress in which, maximum principal stress increases to reach the failure surface ( $\sigma_{1f}$ ). In this condition circle with radius of  $r_C$  represents the stress state at failure. With this loading history, “stress level, SL” is defined as the ratio of radius of current stress level to radius of stress level at failure:

$$SL = \frac{r_A}{r_C} = \frac{\sigma_3 - \sigma_1}{\sigma_3 - \sigma_{1f}} \quad [3]$$

Where:

$$\sigma_{1f} = \frac{1 + \sin \varphi}{1 - \sin \varphi} \sigma_3 - 2c \sqrt{\frac{1 + \sin \varphi}{1 - \sin \varphi}} \quad [4]$$

In these equations inverse of SL is considered to be the local factor of safety in the stress path with constant minimum stress.

Another stress path is defined with constant mean stress and stresses are changed to experience shear failure. Circle with radius  $r_B$  in Fig. 1 will represent the ultimate stress state in this case. The ratio of  $r_A$  to  $r_B$  is defined as over-stress ratio (OSR) (Farias and Naylor [7]), which can be calculated

from:

$$OSR = \frac{r_A}{r_B} = \frac{\sigma_3 - \sigma_1}{-(\sigma_1 + \sigma_3) \sin \varphi + 2c \cos \varphi} \quad [5]$$

Inverse of OSR is defined as local factor of safety for stress path with constant mean stress.

None of the above relations are applied in the strength reduction technique. Instead, in this method, strength parameters are decreased until failure mechanism occurs in the slope. When strength is decreased, yield surface shrinks. Therefore, current stress state may be outside of the yield surface. Due to this situation, unbalanced forces are induced in each node of the finite element model, which must be applied to the next step of calculation. Thus in this method, additional forces due to strength reduction are generated which gradually result in instability.

In the strength reduction technique, local factor of safety can be calculated by putting the failure line on the circle of stress state (Fig. 1). In this condition, local factor of safety can be calculated from:

$$FS(SR) = \sqrt{\alpha^2 - 2\alpha \tan \varphi} \quad [6]$$

Where:

$$\alpha = \frac{2(\sigma_1 \tan \varphi - c)}{\sigma_1 - \sigma_3} \quad [7]$$

With this definition, the new failure envelope passes through  $\sigma_{max} = c/\tan \varphi$  similar to the initial failure envelope.

Therefore, with above definitions, one can calculate local factor of safety for each element in the numerical analyses. It should be mentioned that each point of the model has its value of stress level, overstress ratio and local factor of safety from the strength

reduction technique.

### 3- Closed-form solution for stability analysis

Hoek and Bray [8] presented equation (8) for stability analysis of rock slope which is shown in Fig. 2. In the following equations,  $\gamma$  is unit weight of rock slope, H is height of slope, Z is tension crack depth, B is tension crack horizontal distance from the toe slope and  $\theta$  is angle of discontinuity.

$$FS = \frac{2c/(\gamma H) * P + Q \tan \varphi / \tan \theta}{Q} \quad [8]$$

Where:

$$P = (1 - Z/H) / \sin \theta \quad [9]$$

If tension crack occurs at side R, then:

$$Q = ((1 - (Z/H)^2) / \tan \theta - 1 / \tan \alpha) \sin \theta \quad [10]$$

If tension crack occurs at side L, then:

$$Q = (1 - Z/H)^2 \cos \theta (\tan \alpha / \tan \theta - 1) \quad [11]$$

The critical tension crack depth can be found by minimising the equation (8) with respect to Z/H. This gives the critical tension crack depth equal to:

$$Zc/H = 1 - 1/\sqrt{\tan \theta / \tan \alpha} \quad [12]$$

The corresponding position of tension crack is:

$$Bc/H = 1/\sqrt{\tan \alpha \tan \theta} - 1/\tan \alpha \quad [13]$$

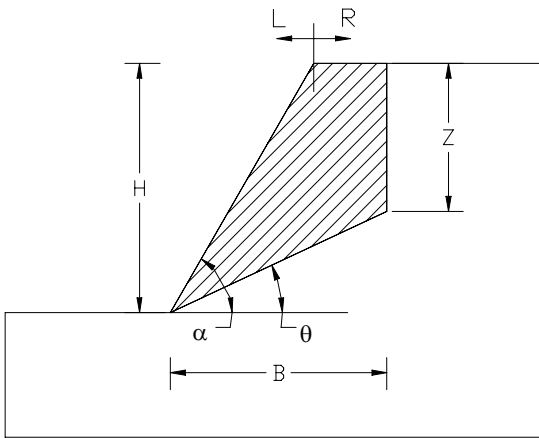


Fig. 2. Parameters used in closed-form analysis

These equations are used for comparison with the safety analysis with the strength reduction technique.

#### 4- Numerical modeling

In this study, analyses are carried out using finite element code (Owen and Hinton [9]). Authors have added one option for modeling the behavior of rock masses with visco-plastic multilaminate framework, which was introduced by Zienkiewicz and Pande [10]. In this method the overall deformation behavior of rock mass can be determined from interaction of joint planes and the intact rock. The following assumptions are required in the formulation of multilaminate framework [11]:

a) All joints in a set are parallel, continuous and unfilled.

b) The volume occupied by the joint sets is small compared to the total volume of the rock mass.

Elastic parameters of intact rock and normal and shear stiffness of rock joints contribute in elastic response of the rock mass. The inelastic strain rate obeys the Perzyna visco-plastic material law [12], where the visco-plastic strain rate is defined by:

$$\dot{\varepsilon}^{vp} = \langle \phi(F^n) \rangle \frac{\partial Q}{\partial \sigma} \mu \quad [14]$$

In the above equation  $\mu$  is fluidity parameter and  $\phi(F^n)$  is Perzyna power function.  $F$  and  $Q$  are yield and potential functions, respectively.  $\langle F \rangle$  is Heviside function of  $F$  and has the following definition:

$$\langle F \rangle = \begin{cases} 0 & F < 0 \\ F & F \geq 0 \end{cases} \quad [15]$$

In this study, power function is assumed the same as the yield function. This equation is applied to the intact rock and rock joints both, for calculating the visco-plastic strain rates. Visco-plastic strain rate of each joint plane is calculated in the local coordinate of that plane. For instance stress state  $\{\sigma\}$  at each integration point of the finite element mesh is transformed into normal and shear stresses  $(\sigma_n, \tau)$  on each joint plane using a transformation matrix  $[T_\sigma]$ :

$$\begin{Bmatrix} \sigma_n \\ \tau \end{Bmatrix} = [T_\sigma] \{\sigma\} \quad [16]$$

Using these transformed stresses, the yield criterion and equation 14, visco-plastic normal and shear strain rates  $(\dot{\varepsilon}^{vp}, \dot{\gamma}^{vp})$  are obtained in the local coordinate system. These local strain rates are transformed to global strain rates with transformation matrix  $[T_\varepsilon]$ :

$$\{\dot{\varepsilon}^{vp}\} = [T_\varepsilon] \begin{Bmatrix} \dot{\varepsilon}_j^{vp} \\ \dot{\gamma}_j^{vp} \end{Bmatrix} \quad [17]$$

Total visco-plastic strain rate of the rock mass is the summation of visco-plastic strain rates of rock joints and intact rock [11]:

$$\dot{\varepsilon}^{VP} = \dot{\varepsilon}_r^{VP} + \dot{\varepsilon}_j^{VP} \quad [18]$$

Finally visco-plastic strain increment is calculated by multiplication of time step  $\Delta t$  by visco-plastic strain rate as follows:

$$\varepsilon^{VP} = \dot{\varepsilon}^{VP} \times \Delta t \quad [19]$$

Summation of visco-plastic strain increment and the elastic strain results in the global strain increment in each load increment. Total strain can be calculated from addition of this strain increment to the previous strain. Yield may occur in either intact rock or along the joint planes, or both, depending on the stress state, orientation of the joint planes and the material properties of the intact rock and joint planes. Different yield function can be defined for joint planes or intact rock; but in this study, both intact rock and joint planes follow Mohr-Coulomb failure criterion with their strength parameters. Associated and non-associated flow rules are applicable in shear failure but only associated flow rule is used in tension.

In the joint planes, following yield and plastic potential functions in shear and tension are defined:

$$F_s = \tau + \sigma_n \tan \varphi_j - c_j, \quad [20a]$$

$$Q_s = \tau + \sigma_n \tan \psi_j$$

$$F_t = \sigma_n - \sigma_j^t \quad Q_t = \sigma_n \quad [20b]$$

Where  $c_j$ ,  $\varphi_j$ ,  $\psi_j$  and  $\sigma_j^t$  are cohesion, friction angle, dilation angle and tensile strength of rock joints, respectively.

There is a limitation for tensile strength in joints which is defined as:

If,

$$\sigma_j^t > c_j / \tan(\varphi_j)$$

then

$$\sigma_j^t = c_j / \tan(\varphi_j) \quad [21]$$

For identifying the factor of safety, shear

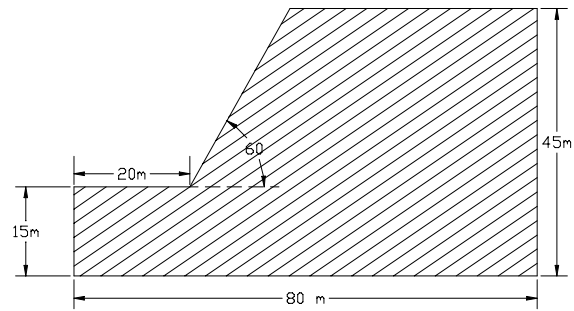


Fig. 3. Dimensions of the slope for safety analysis

strength parameters of intact rock and joint sets are decreased with a factor  $F$ , and then static analysis is performed. If whole system of equations converges, then factor  $F$  is increased in the next analysis. Then new analysis is performed with these reduced parameters. This procedure continues until instability occurs in the model.

It has to be mentioned that in this study, strength reduction technique is modified for considering the effect of tensile strength and dilation angle on the stability of slopes. For instance, tensile strength of rock and joints should be reduced with pre-defined factor  $F$ . Also when elasto-plastic formulation is used, it is recommended to have associated flow rule to reduce the mesh dependency. For more clarification, each of above modification is discussed clearly in separate section.

In this paper, analyses are based on a two-dimensional model with joint strike perpendicular to the plane of analysis. These analyses are performed on an example of rock slope dipping down with the angle of  $60^\circ$ . The dimensions of the slope are shown in Fig. 3. Rock material and joint sets have parameters included in Table 1. In this table,  $E$  is Young's modulus,  $\nu$  is Poisson's ratio,  $\gamma$  is unit weight,  $c$  is cohesion,  $\sigma_t$  is tensile strength,  $\varphi$  is friction angle and  $\psi$  is dilation angle.

Table 1. Properties for stability analysis

Material \ Properties	E (GPa)	$\nu$	$\gamma$ (kN/m <sup>3</sup> )	c (MPa)	$\sigma_t$ (MPa)	$\phi$ (°)	$\psi$ (°)
Rock Material	10	.2	24	3	3	40	40
Rock Joints	-	-	-	0.2	0.2	30	30

### 5- Stability analysis of homogeneous slope

When the number of joint sets increases and the joint sets tend to cover the whole spectrum of dip angles, the system of jointed rock mass tends to exhibit a homogeneous behavior like soil. Thus for simplicity in considering the previous definitions for local factors of safety, a homogeneous rock slope with strength parameters equal to joint strength parameters is considered. For determining the factor of safety only solid matrix with Mohr-Coulomb model is used in the multilaminate framework and results are compared with limit equilibrium method. Limit equilibrium stability analysis is carried out using program STABLE with modified Bishop method (Siegel [13]).

Deformation field of the model after stability analysis is shown in Fig. 4(a). It is obvious that instability occurs from the toe of slope and continues to the top of the slope. Factor of safety from the strength reduction technique is 2.4, which is very near to its value from the limit equilibrium method (2.55).

Fig. 4(b) shows shear strain concentration from the strength reduction technique, which is compared with critical surface of the limit equilibrium method. As it is shown, the results of numerical method are very close to results of equilibrium stability analysis.

For comparing the results of local factor of safety, which was discussed in section 2, point A in Fig. 4(a) is selected, which is in the

critical slip surface. Changes of local factors of safety in this point during the analysis are shown in Fig. 5. In this figure, local factors of safety from inverse of stress level (1/SL) and over-stress ratio (1/OSR) are compared with local factor of safety from the strength reduction technique. Changes in local factors of safety are due to changes in stress state during analysis. It should be mentioned that local factor of safeties in this figure are calculated from stress state in each step of analysis and real value of strength parameters (not reduced parameters); thus each definition for the factor of safety reaches to its own real value of factor of safety in ultimate steps.

Regions of lowest local factor of safety for all definitions are similar and are shown in Fig. 4(b). It is shown that lowest factors of safety produce a region, which is very close to both maximum shear strain concentration contour from numerical method and critical surface from the limit equilibrium analysis.

### 6- Slope stability in jointed rock mass

In this section, Mohr-Coulomb associated flow rule with tension cut-off is considered for intact rock and joint sets. For calculating the factor of safety, strength parameters of intact rock and joint sets are decreased during analysis to reach instability condition.

For evaluation of stability condition, jointed rock slope with corresponding parameters shown in Table 1 is investigated. Joint sets are parallel and have an orientation equal to

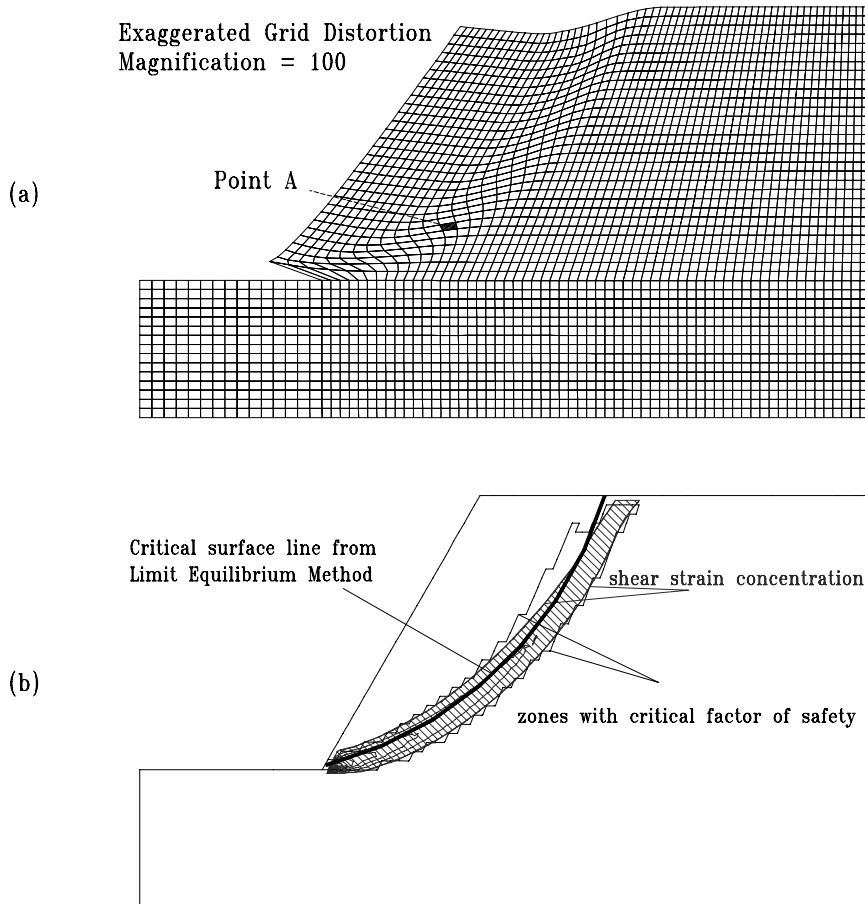


Fig. 4. (a) Grid deformation and (b) failure surface in homogeneous slope

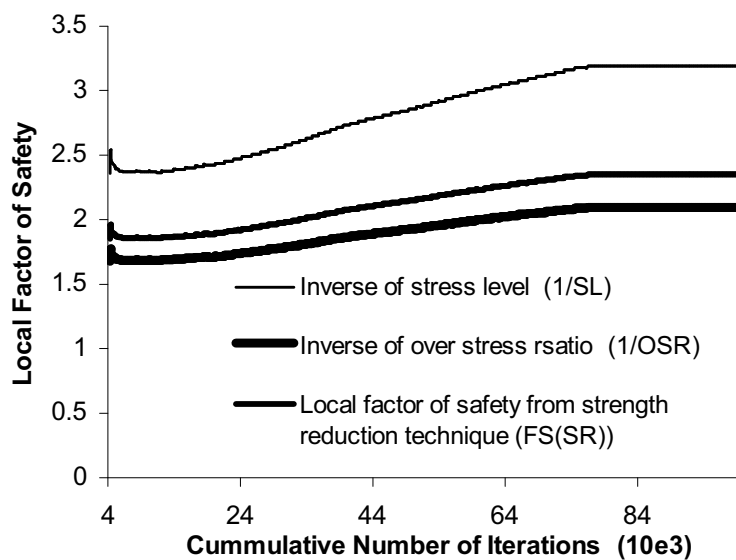


Fig. 5. Changes in local factors of safety at point A during the analysis

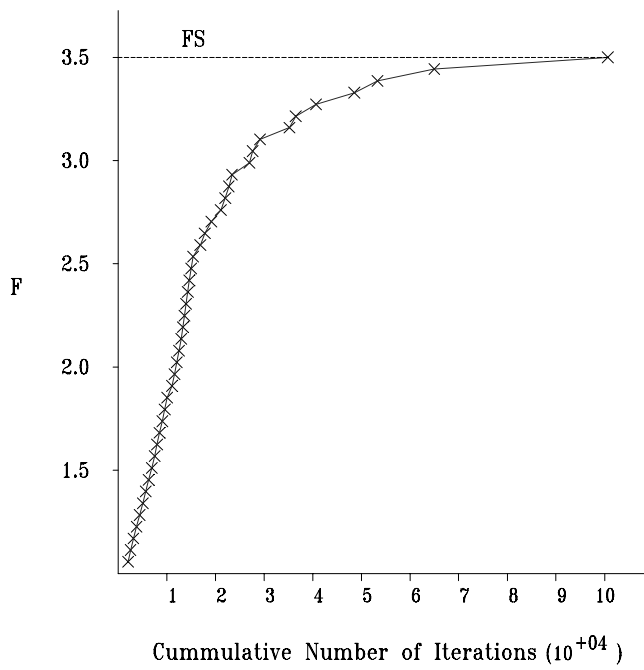


Fig. 6. Changes in factor F in one analysis of jointed rock slope

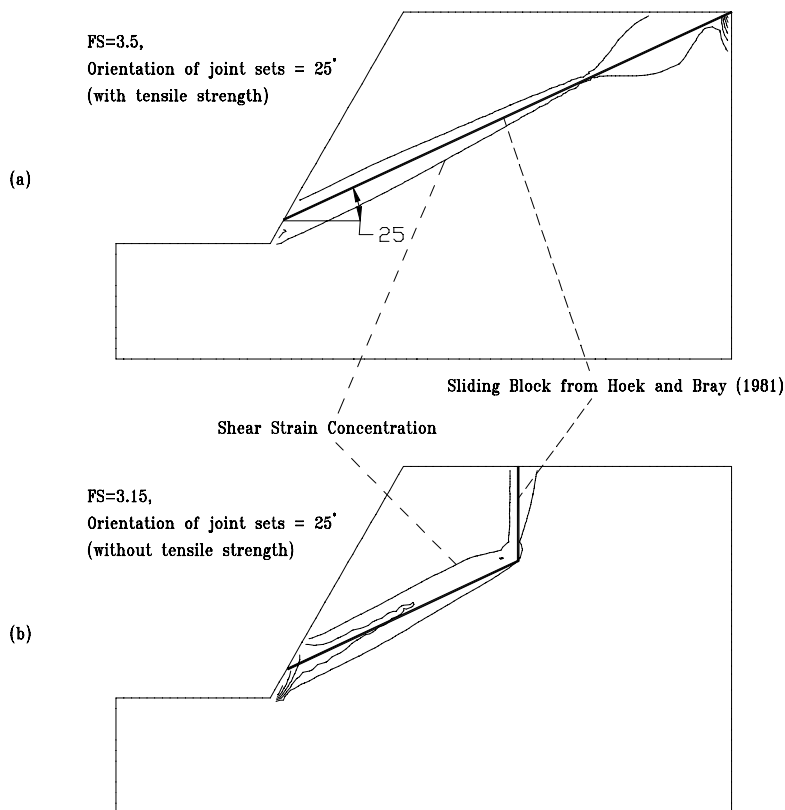


Fig. 7. Slope stability on a layered rock mass, (a) with large tensile strength (b) without tensile strength

25° respect to horizontal axis. First, tensile strength of material is considered very large to avoid any tension crack in the developed sliding block. Increasing the factor  $F$  during the analysis is shown in Fig. 6. As it mentioned before, with increase of factor  $F$ , cohesion and friction angle are decreased with equation 1. It is shown that  $F$  increases during analysis to reach maximum value, which is the real factor of safety. After this value, whole system begins to fail. It is noticeable that when factor  $F$  reaches to the value of factor of safety, model will need large amount of iterations for convergency. Shear strain concentration in this analysis is shown in Fig. 7(a). Factor of safety for this slope is 3.5, which is very near to factor of safety from closed-form solution (3.57) based on the prescribed sliding surface in Fig. 7(a). It should be mentioned that concentrated shear strain in numerical method starts at a location just above the toe of the slope. In the studies of Pande et al [11], the region of maximum shear strain is located about 0.1H above the toe, which is in agreement with this study.

In the following, effects of joint sets parameters are studied on the stability of rock slopes. Effects of cohesion and friction angle are known, therefore, the effect of geometry of joint sets, tensile strength and dilation angle are investigated.

### 6-1- Effect of orientation of joint sets

Orientation of the joint set is defined by dip-direction and dip-angle of the joint surface in plane perpendicular to the strike. For investigating the effect of orientation of joint sets on the factor of safety of slope, orientation of joint sets has been changed from 0 to 90° and corresponding factors of safety in rock slope with these orientations

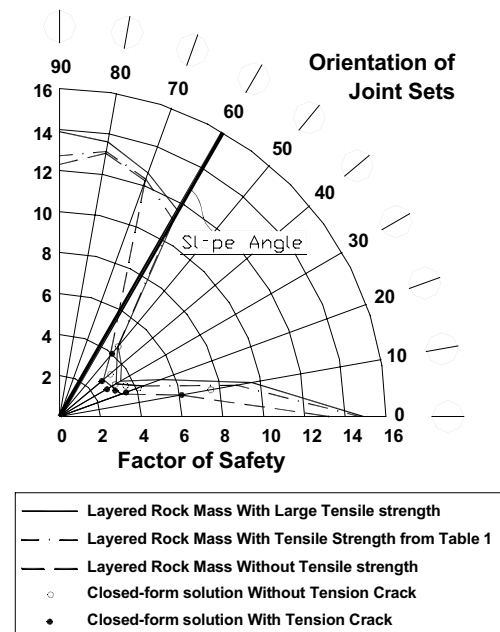


Fig. 8. Rose diagram for factor of safety

are calculated. In Fig. 8 changes in factor of safety with changes in the orientation of joint sets are shown in a rose diagram. As shown in this figure, minimum factor of safety is obtained when orientation of joint sets is between 20 to 50 degrees. At this condition, shear failure on the joint surface is essential cause for reduction of factor of safety. Maximum factor of safety occurs when joint sets are either horizontal or vertical. In these conditions, large factor of safety is due to the strength of intact rock. Maximum factor of safety of slope without joint sets is 23.4. This is even greater than the factor of safety when horizontal joint sets exist. Because in horizontal joint sets, one part of failure surface passes exactly from horizontal layer that has very low shear strength. For comparison, results of stability analysis with Hoek and Bray's equations are shown in Fig. 8 (closed-form solution without tension crack). It can be seen that the results are close to the results of the numerical method. It should be mentioned that if orientation of

joint sets is greater than slope angle, factor of safety can not be calculated from Hoek and Bray's method. For this reason, closed form solution is not shown in the figure for orientation greater than 50°. Also, if joint set orientation is less than a limit value, here 25°, constraint of right boundary in the model affects the numerical results; consequently, factor of safety is not calculated correctly. Thus for stability calculation, boundary of model must be large enough until failure surface doesn't pass through the boundaries. It should be mentioned that the model is not capable of considering the toppling failure, which is very important in the rock masses with vertical or near vertical joint sets. For considering this kind of failure, bending rigidity of layers has to be included in the model, otherwise the homogenized model may considerably overestimate the deformation

### 6-2- Effect of tensile strength on the factor of safety

When tensile strength of rock and joint sets are very low, tension crack occurs on the slope, which leads to lower factor of safety. To obtain the factor of safety and appropriate location of tension crack, it is recommended to reduce the tensile strength during the analysis by the strength reduction technique as follows:

$$\sigma_t^i = \sigma_t^i / F \quad [22a]$$

$$\sigma_t^j = \sigma_t^j / F \quad [22b]$$

Where  $\sigma_t^i$  and  $\sigma_t^j$  are tensile strength of rock and joint sets, respectively.

When the sliding block starts to move along the critical surface, stresses in the upper part of slide reduces until tension stresses occur in

this region. If tensile stresses are greater than tensile strength of materials, these points start to yield on the tension yield surface. Then tensile strain occurs in the upper part of the slope, which is the source of generation of tension crack.

Results of safety analyses with the strength reduction technique for rock mass with tensile strength written in Table 1 are shown in Fig. 8. The values of factor of safety are a little lower than previous study because tensile crack occurs in the sliding block.

Tension crack appears in the slope face according to tensile strength of the intact rock and joint sets. Lowest factor of safety of slope will be in a condition that both intact rock and joint sets have no tensile strength. Thus for comparing the location of tension crack in the rock mass with Hoek and Bray's equations, tensile strength in both joint sets and intact rock is assumed zero in the numerical analysis. The sliding blocks from Hoek and Bray's equations and shear band occurred from the strength reduction technique for dip angle equal to 25° are shown in Fig. 7(b). Shape of sliding block (depth and place of tension crack) in both analyses are very similar.

Results of the factor of safety from Hoek and Bray's equation with tension crack are shown in Fig. 8 for orientation between 10 to 50 degrees (filled points). It is obvious that these values are very close to the results of the strength reduction technique.

### 6-3- Effect of addition of joint sets on the factor of safety

In this part effect of two and three joint sets on the factor of safety is discussed. Different parameters can be applied in each joint set, but here all parameters are equal for all joint sets. In Fig. 9 factors of safety for one joint

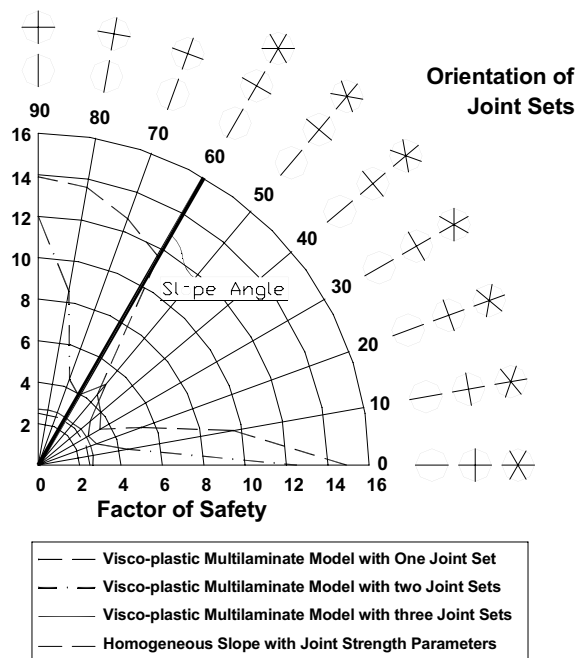


Fig 9. Effect of the number of joint sets on factor of safety

set, two joint sets perpendicular to each other and three joint sets with 60 degrees between them are shown. Factor of safety for two perpendicular joint sets is less than that for one joint set. Also, the factor of safety for 3 joint sets is less than that for two perpendicular joint sets. It is obvious that addition of more joint sets with another orientations results in further reduction in the factor of safety and the factor of safety gradually tends to become a unique value when the jointed rock mass behaves like a homogeneous material.

#### 6-4- Effect of dilation on the factor of safety

Significance of soil dilatancy in the analysis of the slope stability was studied by Rowe [14]. He introduced a stress-dilatancy model and compared its results with traditional Mohr-Coulomb model. He found that the

results obtained by traditional Mohr-Coulomb parameters may err on the unsafe side. Chen [15] proved that collapse loads for a material with non-associated flow rule are smaller than those obtained for the same material with associated flow rule. Vermeer and Deborst [16] showed that use of an associated flow rule leads to an overestimation of the stiffness and load-carrying capacity.

If a soil slope with a specific friction angle is used, higher values of a dilation angle generally leads to larger stability numbers for the same friction angle (Manzari and Nour [17]). Because the limit equilibrium stability analyses are based on the assumption of equality of dilation and friction angle (normality condition), therefore these slope stability analyses are not conservative for granular soil and rock joints that exhibit a dilation angle smaller than a friction angle.

When there is significant difference between friction and dilation angles, loss of ellipticity and instability in constitutive relations occurs, which may lead to ill-posedness and non-uniqueness of the results. Thus results will be mesh dependent. This problem happens in elasto-plastic analysis, when shear band develops in the medium. Even using the shear strength reduction technique with an associated flow rule, elasto-plastic stress-strain analysis may lead to non-uniqueness in the results; because in this analysis, cohesion and friction angle decreases during the analysis, which is a kind of softening phenomenon. This non-uniqueness can be avoided by some method such as considering the plastic deformation to be a limit state of visco-plastic behavior. This process is known as regularization (Zienkiewicz and Taylor [18]).

In this study, because of using visco-plastic approach in the multilaminar model, mesh

Table 2. Effect of dilation on factor of safety

Dilation Angle at joint (deg.)	0	10	20	30
Factor of Safety	3.44	3.45	3.46	3.48

dependency will be reduced in the stability analyses. Also in this method, due to using initial stiffness method, ill-posedness will not occur in the constitutive relations.

In rock joints at low normal stresses, dilation angle increases the shear strength of joints. Thus, increasing the dilation angle results in increasing strength parameters. But in this paper, shear strength is assumed to be constant and only changes in the dilation angle are studied (due to the flow rule in equation 14, variation of dilation angle leads to variation in the volumetric strain; Thus dilation angle has no direct effect on the shear strength parameters).

The strength reduction technique is used for stability analysis of jointed rock slope with orientation of 25°. Intact rocks usually have associated behavior. For this reason, sensitivity analyses are performed with changes in the joint dilation angle. The results of these analyses with different dilation angles are shown in Table 2. It is shown that with increasing dilation angle with constant friction angle, the factor of safety increases but the changes are very small.

It should be mentioned that the problem, which introduced here is in CNL condition (Constant Normal Load on joints). In CNS condition (Constant Normal Stiffness), the dilation angle leads to increasing in strength of material. In this condition, increasing in dilation angle causes increasing in normal stress, consequently shear strength is

increased (Indraratna and Haque [19]). For example when a shear displacement occurs in a prestressed rock joints with bolts, dilation angle leads to have a normal displacement and due to elastic behavior of bolts, normal stress on joint is increased.

In the stability analysis of slopes with elasto-plastic procedure, mesh dependency of results can be reduced when dilation angle  $\psi$  decreases similar to friction angle:

$$\tan\psi' = \tan\phi' = \tan\phi / F \quad [23]$$

In this condition, flow rule will be associated throughout the process and mesh dependency occurs only due to reduction of shear strength parameters.

## 7- Conclusions

The stability of a jointed rock slope has been studied with the strength reduction technique. Visco-plastic multilaminate framework is used for stability analysis. Results of the numerical analyses are compared with the results of the limit equilibrium method. It has been demonstrated that the location of the sliding surface and the value of factor of safety from the strength reduction technique are in good agreement with the limit equilibrium method. Factor of safety for one joint set is calculated with changes in orientation of joint sets from 0 to 90°. It was shown that the factor of

safety in joint sets with horizontal and vertical orientations is maximum.

Effect of tensile strength of rock and joint sets was investigated in the analyses. In this condition, it is recommended that tensile strength of rock and joints to be decreased during the analyses like cohesion and friction. It was shown that the strength reduction technique can accurately show the location of tension crack in rock slope which is approximately equal to closed-form solution.

Effect of joint dilation angle was also investigated on the factor of safety. It is shown that with a constant friction angle, with increasing in the dilation angle, factor of safety increases slightly.

## References

1. Zienkiewicz, O.C., Humpheson, C., and Lewis, R.W. 1975. "Associated and non-associated visco-plasticity and plasticity in soil mechanics," *Geotechnique*, 25(4): 671-689.
2. Naylor, D.J. 1982. "Finite elements and slope stability," In *Numerical Methods in Geomechanics*, D.Reidel Publishing Company. pp. 229-244.
3. Matsui, T., and San, K. C. 1992. "Finite element slope stability analysis by shear strength reduction technique," *Soils and Foundations*, 32(1): 59-70.
4. Lane, P.A., and Griffiths, D.V. 1997. "Finite element slope stability analysis-Why are engineers still drawing circles?," In *Numerical Models in Geomechanics*, Balkema, Rotterdam. pp. 589-593.
5. Dawson, E.M., Roth, W.H., and Drescher, A. 1999. "Slope stability analysis by strength reduction," *Géotechnique*, 49(6): 835-840.
6. Rachez, X., Billiaux, D., and Hart, R. 2002. "Slope stability analysis with integrated shear strength reduction algorithm," In *Numerical Methods in Geomechanical Engineering*, Presses de l'ENPC/LCPC, Paris, pp.731-736.
7. Farias, M. M., and Naylor, D. J. 1998. "Safety analysis using finite elements," *Computer and Geotechnics*, 22(2): 165-181.
8. Hoek, E., and Bray, J. 1981. *Rock slope engineering*. Institute of Mining and metallurgy, London.
9. Owen, D.R.J., and Hinton, E. 1980. *Finite elements in plasticity: Theory and practice*, Pineridge press limited.
10. Zienkiewicz, O.C., and Pande, G.N. 1977. "Time dependent multilaminate model of rocks - a numerical study of deformation and failure of rock masses," *International Journal for Numerical and Analytical Methods in Geomechanics*, 1: 219-247.
11. Pande, G.N., Beer, G. and Williams, J.R. 1990. *Numerical Methods in Rock Mechanics*. John Wiley & Sons LTD.
12. Perzyna, P. 1966. "Fundamental problems in viscoplasticity," *Advances in Applied Mechanics*, 9, 243-377.
13. Siegel, R.A. 1975. *Stable user manual*. A program for analysis of general slope

- stability problem. Purdue University.
14. Rowe, P.W. 1963. "Stress-dilatancy, earth pressure and slopes," *Journal of Soil Mechanics and Foundation Engineering*, ASCE, 89(5): 37-61.
  15. Chen, W.F. 1975. *Limit analysis and soil plasticity*. Elsevier Science, Amsterdam.
  16. Vermeer, P.A., and Deborst, R. 1974. "Non-associated plasticity for soils, concrete and rock." *Heron*, 29(3).
  17. Manzari, M.T., and Nour, M.A. 2000. "Significance of soil dilatancy in slope stability analysis," *Journal of Geotechnical and Geoenvironmental Engineering*, ASCE, 126(1), 75-80.
  18. Zienkiewicz, O.C., and Taylor, R.L. 2000. *The finite element method*. Fifth edition, Butterworth-Heinemann.
  19. Indraratna, B., and Haque, A. 2000. *Shear behavior of rock joints*. Balkema/ Rotterdam/Brookfield.